Environmental Science & Technology

Article

Cite This: Environ. Sci. Technol. 2018, 52, 11223−11231

pubs.acs.org/est

Ammonia Emission Measurements for Light-Duty Gasoline Vehicles in China and Implications for Emission Modeling

Cheng Huang,*[,†] Qingyao Hu,[†] Shengrong Lou,[†] Junjie Tian,[‡] Ruining Wang,[§] Chong Xu,[§] Jingyu An,[†] Hongjuan Ren,[§] Dong Ma,[∥] Yifeng Quan,[⊥] Yaojiao Zhang,[⊥] and Li Li*[,†,¶]

[†]State Environmental Protection Key Laboratory of Cause and Prevention of Urban Air Pollution Complex, Shanghai Academy of Environmental Sciences, Shanghai, 200233, China

[‡]School of Resources and Environment Engineering, East China University of Science and Technology, Shanghai, 200237, China

[§]Automotive Engineering College, Shanghai University of Engineering Science, Shanghai, 201620, China

[∥]Chinese Research Academy of Environmental Sciences, Beijing, 100012, China

[⊥]Shanghai Motor Vehicle Inspection Certification & Tech Innovation Center Co., Ltd, Shanghai, 201805, China

Supporting Information

ABSTRACT: Motor vehicle ammonia (NH_3) emissions have attracted increasing attention for their potential to form secondary aerosols in urban atmospheres. However, vehicle NH_3 emission factors (EFs) remain largely unknown due to a lack of measurements. Thus, we conducted detailed measurements of NH_3 emissions from 18 Euro 2 to Euro 5 light-duty gasoline vehicles (LDGVs) in Shanghai, China. The distance- and fuel-based NH_3 EFs average 29.2 ± 24.1 mg·km^{-1} and 0.49 ± 0.41 g·kg^{-1}, respectively. The average NH_3-to-CO_2 ratio is 0.41 ± 0.34 ppbv·ppmv^{-1}. The measurements reveal that NH_3 emissions from LDGVs are strongly correlated with both vehicle specific power (VSP) and the modified combustion efficiency (MCE); these relationships were used to predict LDGV NH_3 EFs via a newly developed model. The predicted LDGV NH_3 EFs under urban and highway driving cycles are 23.3 mg·km^{-1} and 84.5 mg·km^{-1}, respectively, which are consistent with field measurements. The NH_3 EF has decreased by 32% in average since the implementation of vehicle emission control policies in China five years ago. The model presented herein more accurately predicts LDGV NH_3 emissions, contributing substantially to the compilation of NH_3 emission inventories and prediction of future motor vehicle emissions in China.

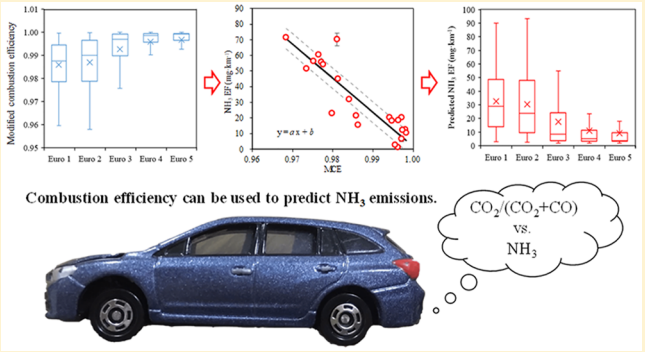

INTRODUCTION

Ammonia (NH_3) is an important atmospheric alkaline species. NH_3 reacts with nitric and sulfuric acids to form nitrate and sulfate aerosols, which degrade regional air quality.[1−3] Agricultural activities, such as livestock breeding and NH_3-based fertilizer application, are the dominant sources of NH_3 emissions at regional and global scales.[4−7] However, recent work has revealed that NH_3 emissions from vehicles, which are an important NH_3 source in urban areas,[8,9] contribute more than agricultural sources to secondary aerosol formation during haze pollution events in urban Beijing, China.[10] Gasoline vehicles equipped with three-way catalytic converters (TWCs), which generate NH_3 during the catalytic reduction of nitric oxide (NO) via the water−gas shift reaction, are the major contributor to vehicular NH_3 emissions.[11] Unlike conventional pollutants such as CO, nitrogen oxide (NO_x), total hydrocarbons (THCs), etc., NH_3 emissions from gasoline vehicles are currently not regulated. Recent remote sensing studies in the United States indicate that ratios of NH_3 emissions to reactive nitrogen emissions are rapidly increasing.[13]

NH_3 emission factors (EFs) were initially determined for entire vehicle fleets under real-world conditions via tunnel experiments.[14−16] Subsequent laboratory dynamometer studies have been conducted in the past decade to determine NH_3 EFs for individual vehicles.[17−23] Dynamometer results indicate that vehicular NH_3 emissions depend strongly on vehicle operation and characteristics, such as driving cycle, Vehicle Specific Power (VSP), and vehicle age. Such studies are important for the development of vehicular NH_3 emission inventories. However, quantitative studies on NH_3 emissions from vehicles in China remain limited. Liu et al.[24] and Chang et al.[8] reported NH_3 EFs from on-road vehicles in tunnel experiments in 2014 and 2016, respectively, but the EFs therein differed by nearly a factor of 10. Sun et al.[9,25] measured fleet-integrated NH_3 emissions using a mobile laboratory in six cities in China

Received: July 19, 2018
Revised: August 29, 2018
Accepted: August 30, 2018
Published: August 30, 2018

DOI: 10.1021/acs.est.8b03984
Environ. Sci. Technol. 2018, 52, 11223−11231

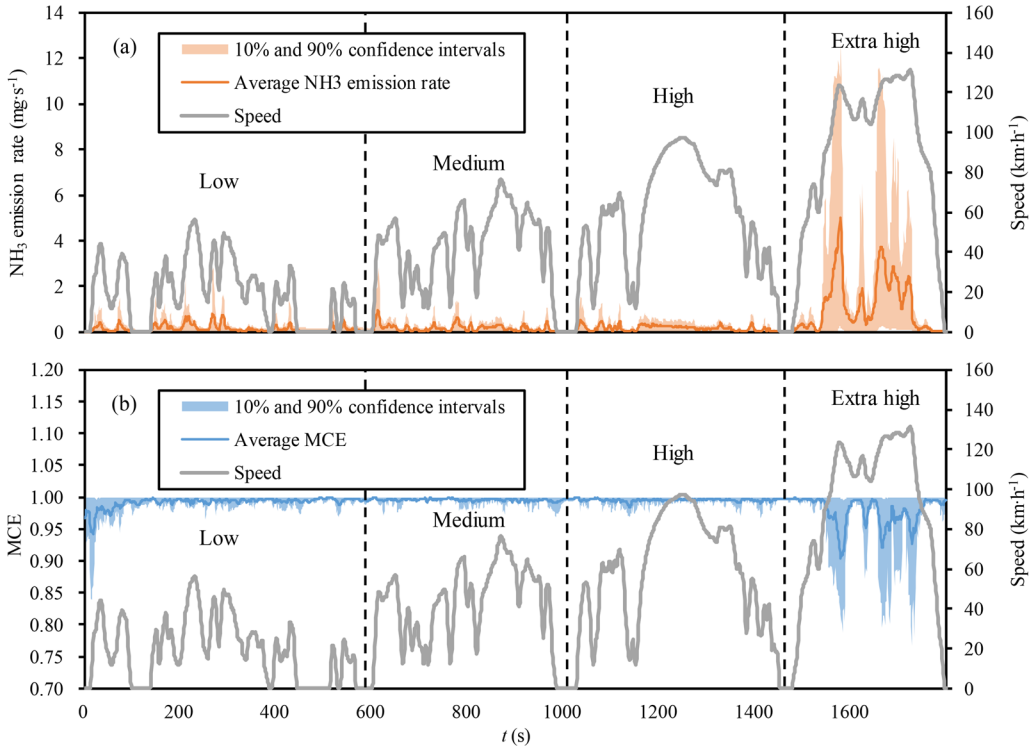

Figure 1. (a) Instantaneous NH_3 emission rates and (b) modified combustion efficiencies (MCEs, equal to $\Delta[CO_2]/(\Delta[CO_2] + \Delta[CO])$) under hot-start conditions during the WLTC. Solid lines represent average values from the test vehicles. Shaded areas represent 10% and 90% confidence intervals.

and the United States, observing that NH_3 emissions from on-road vehicles were higher in Chinese cities than in U.S. cities, especially for Chinese cities with less stringent standards. Vehicle emission models, such as MOVES, COPERT, IVE, etc., can be used to estimate NH_3 emissions from vehicles. Nonetheless, the accuracy of vehicular NH_3 emission model results remains in question due to the lack of experimental verification in China, leading to large uncertainties in transportation sector NH_3 emission inventories.[5,26−29]

The number of motor vehicles in China has grown rapidly in recent years, reaching 184 million in 2016, of which 163 million (88.5%) were light-duty gasoline vehicles (LDGVs), representing a 16% increase over the previous year.[30] Rapid increases in the vehicle fleet will probably lead to higher NH_3 emissions in urban areas in China. It is therefore essential to understand local NH_3 emissions from gasoline vehicles in China. Moreover, previous studies have not quantified the relationships between vehicular NH_3 emissions and vehicle performance and characteristics. Further research is needed to improve NH_3 emissions modeling for LDGVs with diverse driving habits, vehicle specifications, and emission standards.

In this study, NH_3 emissions were measured for 18 in-use LDGVs with Euro 2 to Euro 5 emission standards using an extractive diode laser ammonia detection system on a dynamometer chassis. The vehicles were tested via the Worldwide harmonized Light vehicles Test Cycle (WLTC) under cold- and hot-start conditions. The impacts of driving cycle and combustion efficiency on NH_3 emissions were explored in terms of results from this and previous studies. Then, a regression model was established and used to estimate LDGV NH_3 EFs under different driving cycles and combustion efficiencies using large amounts of vehicle inspection data. The results may be used to improve the accuracy of LDGV NH_3 emissions estimations.

EXPERIMENTAL METHODS

Test Vehicles and Fuels. A total of 18 LDGVs were tested in this study, all of which were passenger cars, which constitute more than 99% of the LDGVs in China.[30] The test vehicle model years spanned 2006 to 2016. The accumulated mileages were 23 529−371 935 km and the engine displacements were 1.5−2.3 L. The test fleet consisted of two Euro 2, four Euro 3, eight Euro 4, and four Euro 5 vehicles. China implemented Euro 2, 3, 4, and 5 emission standards in 2004, 2007, 2011, and 2016, respectively. Euro 2−5 vehicles accounted for ∼96% of the gasoline vehicles in China in 2017. Descriptions of the test vehicles are provided in Supporting Information (SI) Section S1. Typical commercial fuel found at gasoline stations in Shanghai was used in the tests herein; this fuel should be in compliance with Euro 5 fuel requirements, which specify that the fuel contain <10 ppm of S, 25% olefins, and 40% aromatics.

Test Procedures. All vehicles were tested on a VULCAN EMSCD48 1.22-m single roll electric chassis dynamometer (Horiba, Japan) at the Shanghai Motor Vehicle Inspection Certification and Tech Innovation Center. Tailpipe emissions were sampled using a constant volume sampling (CVS) system (CVS-7000, Horiba, Japan). Raw exhaust was diluted with high-efficiency particulate air (HEPA)-filtered air in the CVS. Exhaust gas analysis was performed using a Horiba MEXA-7000 measurement system. CO and CO_2 were measured using nondispersive infrared (NDIR) instruments, THCs were measured via flame ionization detection (FID), and NO_x (including NO and NO_2) were measured using a chemiluminescence detector (CLD). The detector deploys with a molybdenum converter to convert NO_2 to NO and measures

DOI: 10.1021/acs.est.8b03984
Environ. Sci. Technol. 2018, 52, 11223−11231

Table 1. NH_3-to-CO_2 Ratios and Distance- and Fuel-based NH_3 EFs from Dynamometer, Tunnel, Remote Sensing, and On-Road Measurements

study	test vehicles	measurement method	analytical method	NH_3 ($mg \cdot km^{-1}$)	NH_3 ($g \cdot kg^{-1}$)	NH_3 to CO_2 ratio ($ppbv \cdot ppmv^{-1}$)
this study	13 (Euro 2−5)	dynamometer (WLTC)	TDL	29.2 ± 24.1	0.49 ± 0.41	0.41 ± 0.34
Suarez-Bertoa et al. (2014)[31]	7 (Euro 5a−6)	dynamometer (NEDC)	FTIR	20.3 ± 19.6		0.31 ± 0.33
Livingston et al. (2009)[23]	41 (Tier 0, Tier 1, TLEV, LEV, ULEV, SULEV)	dynamometer (FTP)	FTIR	41 ± 46		
		dynamometer (UC)	FTIR	58 ± 48		
		dynamometer (SC03)	FTIR	24 ± 16		
		dynamometer (US06)	FTIR	76 ± 82		
		dynamometer (M090)	FTIR	32 ± 28		
Heeb et al. (2008)[21]	10 (Euro 3)	dynamometer (EDC)	CIMS	16 ± 12		
	10 (Euro 4)	dynamometer (EDC)	CIMS	10 ± 7		
Karlsson (2004)[32]	5	dynamometer (NEDC)	SIMS	8.3 ± 7.2		
		dynamometer (FTP)	SIMS	17.3 ± 14.0		
Durbin et al. (2004)[19]	12 (LEV, ULEV, SULEV)	dynamometer (FTP)	TDL	10.7		
		dynamometer (US06)	TDL	52.0		
Durbin et al. (2002)[17]	39 (Tier 0, Tier 1, LEV, ULEV)	dynamometer (FTP)	FTIR	33.6 ± 32.9	0.41 ± 0.12	
Vieira-Filho et al. (2016)[33]	gas-dominated	tunnel	H_2SO_4 absorption	44 ± 22		
Chang et al. (2016)[8]	85% gasoline	tunnel	H_2SO_4 absorption	28 ± 5		
Liu et al. (2014)[24]	88.2% gasoline	tunnel	CLD	230 ± 14	1.79 ± 0.14	
Kean et al. (2009)[16]	∼99% gasoline	tunnel	IC	49 ± 4	0.40 ± 0.02	
Kean et al. (2000)[15]	∼99% gasoline	tunnel	IC	78 ± 6	0.64 ± 0.04	
Fraser and Cass (1998)[14]	>90% gasoline	tunnel	colorimetric	61		
Bishop et al. (2015)[13]	LDV	remote sensing	dispersive UV		0.43−0.80	
Bishop et al. (2010)[12]	LDV	remote sensing	dispersive UV		0.49−0.79	
Burgard et al. (2006)[35]	LDV	remote sensing	dispersive UV		0.50 ± 0.01	
Baum et al. (2001)[34]	LDV	remote sensing	dispersive UV	34 ± 11	0.35 ± 0.03	0.32
Zavala et al. (2006)[36]	LDV	on-road chasing	TILDAS			0.12 ± 0.07
Sun et al. (2017)[9]	LDV in the U.S.	on-road chasing	open-path TDL			0.27−0.40
	LDV in China	on-road chasing	open-path TDL			0.36−0.56

NO. It should be mentioned that a small amount of NOz may be converted to NO by the converter and then accounted as NO_x emissions.

All vehicles were tested over the WLTC, and four vehicles were tested under both cold- and hot-start conditions (see SI Table S1). The WLTC consists of four segments, namely "low-speed", "medium speed", "high-speed", and "extra high-speed". The actual speeds were not allowed to deviate by more than ±2 $km \cdot h^{-1}$ from the driving cycle target speeds more than 10 times during a given test; tests that failed to meet this criterion were suspended. The vehicles were switched off and stored at room temperature (∼10−20 °C) for more than 12 h prior to cold-start testing.

NH_3 Measurements. A variety of measurement instruments, including Fourier Transform Infrared (FTIR),[17,19,23,31] tunable diode laser (TDL),[18,20] chemical ionization mass spectrometer (CIMS),[21,22] and soft ionization mass spectrometer (SIMS)[32] systems, has been used for real-time vehicle NH_3 emission measurements in previous studies. In this study, we used a TDL-based NH_3 measurement system (NMS, IAG Inc., Austria). The analyzer consists of an infrared laser with a 400 mm path length, optical lenses that focus the laser light through the sample gas and then onto a detector, the detector, and the associated electronics, which control the laser and translate the detector signal into a gas concentration. NH_3 typically requires an extended period to equilibrate with instrument walls. To minimize wall losses, the interior surfaces of the instrument are made primarily of stainless steel and polished using a special technology to minimize binding sites; the sampling flow rate was set to 10 $L \cdot min^{-1}$ to improve the response time (1 Hz), and the instrument was equipped with a heated sampling tube that maintained a sample temperature of 191 °C. The analyzer was calibrated with a commercial reference gas (490 ppm of NH_3 in N_2, 4 L cylinder, certified by

DOI: 10.1021/acs.est.8b03984
Environ. Sci. Technol. 2018, 52, 11223−11231

the National Institute of Metrology, China) each day before measurement. The reference gas bias was within 10% at all times. Four LDGVs from the test fleet were used to validate the reproducibility of the measurement system. Detailed analysis is provided in SI Section S2. The results indicate both the instantaneous NH_3 concentrations and emission rate were highly reproducible. During the replicate tests, the relative deviations in the NH_3 EFs were 2.1−16.5%, according to the EFs shown in SI Table S1.

RESULTS AND DISCUSSION

Measurement Results. Instantaneous NH_3 emission rates during the WLTC under hot-start conditions are shown in Figure 1(a). Maximum NH_3 emissions occur primarily during the extra high-speed segment of the WLTC.

Previous studies have indicated that NH_3 emissions from gasoline vehicles with TWCs tend to be higher during fuel-rich combustion, in which the air: fuel equivalence ratio (λ) is relatively low.[18,21] Because λ was not measured, we used the modified combustion efficiency (MCE), which is calculated via $\Delta[CO_2]/(\Delta[CO_2] + \Delta[CO])$, to represent combustion efficiency herein. Figure 1(b) shows instantaneous MCE values during the WLTC. NH_3 emissions are strongly negatively correlated with the MCE. MCE decreases perceptibly during the extra high-speed segment, while NH_3 emissions show corresponding increases.

The MCE is also relatively low during the first 200 s after vehicle ignition; however, NH_3 emissions do not increase, as the TWC is not yet activated during this period due to the low temperature. This feature is more obvious under cold-start conditions; NH_3 emissions in the first 200 s are generally lower after a cold-start than after a hot-start, as shown in SI Figure S2. After 200 s, cold-start NH_3 emissions increase substantially compared with hot-start emissions. After ∼800 s, the NH_3 emissions under the two start-up conditions are similar. Detailed information is provided in SI Section S3.

Test vehicle fuel consumption and distance-based EFs for NH_3 and other gaseous species are summarized in SI Table S1. The methods used to calculate fuel consumption and the EFs are detailed in SI Section S1. The test vehicle NH_3 EFs vary from 1.3 to 73.0 mg·km^{-1} and average 29.2 ± 24.1 mg·km^{-1}. The average fuel-based NH_3 EF is 0.49 ± 0.41 g·kg^{-1} (the gasoline density is assumed to be 0.75 kg·L^{-1}). The average NH_3-to-CO_2 ratio is 0.41 ± 0.34 ppbv·ppmv^{-1}. The EFs of regulated pollutants (e.g., CO, THC, NO_x, etc.) decrease with increasingly stringent emission standards, as shown in SI Figure S3. However, there is no correlation between NH_3 EFs and the emission standards; considerably higher NH_3 EFs are detected for Euro 5 LDGVs, which implies that LDGV NH_3 emissions should be determined by factors other than the emission control technology used in the given vehicle.

Table 1 summarizes the distance- and fuel-based NH_3 EFs and NH_3-to-CO_2 ratios measured in this study and compares these values with previous results obtained from dynamometer, tunnel, remote sensing, and on-road experiments. The distance-based NH_3 EFs from previous dynamometer studies vary from 10 to 76 mg·km^{-1} over a wide range of vehicle technologies and driving cycles; vehicles operated under more aggressive driving cycles, such as the Unified Cycle (UC) and US06, usually have higher NH_3 EFs, which is consistent with our measurements. The NH_3 EFs and NH_3-to-CO_2 ratios herein also agree well with on-road tunnel measurements, remote sensing data, and on-road vehicle chasing results from previous studies. Chang et al.[8] and Sun et al.[9] reported an average NH_3 EF of 28 ± 5 mg·km^{-1} and NH_3-to-CO_2 ratios of 0.36−0.56 ppbv·ppmv^{-1} in cities in China, quite similar to the results measured herein. Tunnel and on-road measurements encompass all types of vehicles, including gasoline and diesel vehicles. However, we believe that the influence of diesel vehicles on NH_3 emissions is limited. First, test tunnels and roads are generally dominated by gasoline vehicles, which account for ∼85−99% of the passing vehicles. In addition, few diesel vehicles in China were equipped with selective catalyst reduction (SCR) systems at the time of the previous studies; vehicles without SCR systems generally have low NH_3 emissions and, thus, little effect on emissions results.[37]

NH_3 Emissions and VSP. VSP, which is defined as the instantaneous power generated per unit mass of the vehicle, is a comprehensive index used to evaluate vehicle engine load, where higher VSP values indicate higher engine load. VSP can be calculated according to Formula 1, as proposed by Jimenez-Palacios:[38]

$$\begin{aligned} \mathrm{VSP} &= v\left[a(1+\varepsilon_i) + g(s + C_R + C_{if}) + \frac{1}{2}\rho_a \frac{C_d \cdot A}{m}(v + v_w)^2\right] \\ &= v(1.1a + 9.81s + 0.132) + 0.302 \times 10^{-3} v^3 \end{aligned} \quad (1)$$

where v is the velocity (m·s^{-1}); a is the acceleration (m·s^{-2}); ε_i is the "mass factor", which is the equivalent translational mass of the rotating components (wheels, gears, shafts, etc.) in the powertrain; g is the acceleration due to gravity (m·s^{-2}; a value of 9.81 m·s^{-2} was used herein); s is the road grade; C_R is the rotational drag coefficient (unitless); C_{if} is the friction coefficient (unitless); ρ_a is the air density (kg·m^{-3}; 1.293 kg·m^{-3} at 20 °C was used herein); C_d is the aerodynamic drag coefficient (unitless); A is the frontal area of the vehicle (m^2); m is the vehicle mass (kg); and v_w is the wind speed (m·s^{-1}). For light-duty vehicles, Jimenez-Palacios[37] recommended the following simplified parameters: ε_i = 0.1, s = 0, C_R = 0.0135, and $C_d \cdot A/m$ = 0.0005; s, C_{if}, and v_w can be neglected. Hence, the equation can be simplified to equal the second part of Formula 1.

VSP has been widely used in emission models to estimate vehicle emissions. Different VSP intervals relate to different operating modes of a vehicle. When VSP < 0 kW·t^{-1}, vehicles are in a state of deceleration. On the contrary, vehicles are in a state of acceleration or cruise speed. When 0 ≤ VSP < 15 kW·t^{-1}, vehicles are usually in low-speed transient or cruising. When VSP ≥ 15 kW·t^{-1}, vehicles are usually running at high speed. The relationship for each test vehicle is provided in SI Section S5. Figure 2(a) indicates that the average NH_3 emission rate is flat when VSP is negative, and then increases with increasing VSP when VSP is positive. NH_3 emissions show two different modes of behavior when VSP > 0 kW·t^{-1}; a slowly upward trend in low-VSP region and a rapidly increasing trend in high-VSP region. Both trends are in linear. The breakpoint between two modes is located at about 15 kW·t^{-1} when vehicle is running at medium-high speed. The correlation between NH_3 emission rate and VSP in this study is consistent with that in Huai et al.[20] Due to the changing slope, we divided the VSP values into three intervals (VSP < 0 kW·t^{-1}, 0 ≤ VSP < 15 kW·t^{-1}, and VSP ≥ 15 kW·t^{-1}) and

DOI: 10.1021/acs.est.8b03984
Environ. Sci. Technol. 2018, 52, 11223−11231

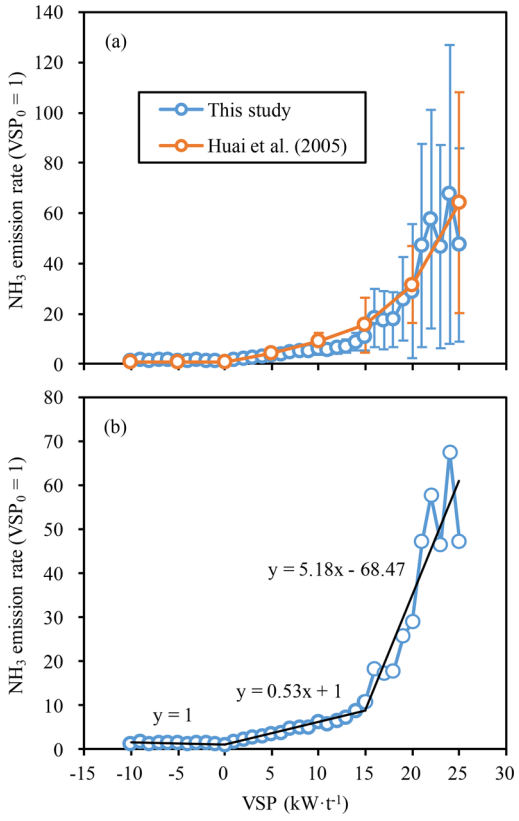

Figure 2. (a) Relationship between NH_3 emission rates and VSP measured herein (blue line) and in Huai et al.[20] (orange line); error bars indicate standard deviations. (b) Piecewise NH_3 emission rate linear regressions (black lines) for the measurements in this study.

calculated a linear regression function for each interval; the regression formulas are shown in Figure 2(b).

NH_3 Emissions and MCE. As discussed above, NH_3 emissions are strongly correlated with the MCE; the associated test vehicle data regression equation is shown in Figure 3. The NH_3 EF generally decreases with increasing MCE. The linear regression yields a slope (average NH_3-to-MCE ratio) of -2054 ± 240 and an R^2 of 0.79, indicating that the MCE can be used to predict the NH_3 EF. The NH_3 in gasoline exhaust is a byproduct of the reduction of NO produced in the engine by the TWC.[39] The MCE is a combination of engine combustion

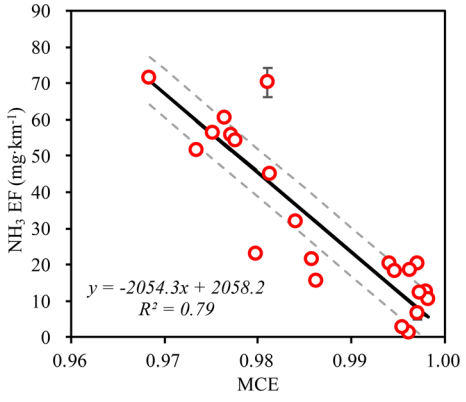

Figure 3. Correlation between test vehicle NH_3 EFs and MCEs. The solid line represents the fitted curve; the dashed lines represent the 5−95% confidence interval.

efficiency and conversion efficiency on the catalyst. Lower MCE value indicates worse combustion efficiency and more original emissions, which will generally induce more NH_3 generation after the catalytic converter. Thus, this correlation implies that improving the combustion efficiency can help to control NH_3 emissions from TWC-equipped LDGVs.

NH_3 Emission Prediction for In-Use LDGVs. Using the correlations between NH_3 EF and VSP and between NH_3 EF and MCE, one can estimate NH_3 emissions from an individual LDGV when the driving cycle, CO EF, and CO_2 EF are known. The NH_3 EF over a given driving cycle can be predicted by Formula 2.

$$EF_i = a \times MCE + b \quad (2)$$

Here, EF_i ($mg \cdot km^{-1}$) is the NH_3 EF over driving cycle i, and a and b are the fit parameters shown in Figure 3. When the driving cycle varies, the NH_3 EF can be predicted by Formula 3.

$$EF_j = EF_i \times \frac{\sum_t (Q_{[t]} \times f_{[t_j]})/\bar{U}_j}{\sum_t (Q_{[t]} \times f_{[t_i]})/\bar{U}_i} \quad (3)$$

where EF_j ($mg \cdot km^{-1}$) is the NH_3 EF for driving cycle j; $Q_{[t]}$ ($mg \cdot s^{-1}$) is the average NH_3 emission rate in VSP bin t, which can be determined using the piecewise linear regression equations shown in Figure 2(b); $f_{[ti]}$ and $f_{[tj]}$ are the fractions of VSP bin t applied in driving cycle i and j; and $\bar{U}_i$ and $\bar{U}_j$ ($km \cdot h^{-1}$) are the average speeds during driving cycles i and j.

MCE data were obtained for 4,048 randomly selected in-use LDGVs from vehicle emission inspection stations in Shanghai and Hangzhou, China; these in-use LDGVs were tested using the vehicle mass analysis system (VMAS) test method, which is widely used in Chinese cities. CO_2 was measured in a one-bag Economic Commission of Europe (ECE) urban cycle test using a nondispersive infrared (NDIR) detector. CO was detected simultaneously via NDIR. The maximum speed in the driving cycle was 50 $km \cdot h^{-1}$, and the average speed was 18.8 $km \cdot h^{-1}$. The MCE was calculated via $EF_{CO2}/(EF_{CO2} + EF_{CO})$. As shown in Figure 4(a), the in-use LDGV MCEs increase with more stringent emission standards. In the last two decades, China has implemented a number of regulations, including new vehicle emission standards, in-use vehicle inspections, and fuel quality improvements. Emissions of regulated pollutants, including CO, THC, and NO_x, from vehicles have been effectively mitigated.[40] Our previous study indicated that CO emissions from Euro 3, 4, and 5 LDGVs are 63%, 90%, and 90% lower than those from Euro 2 vehicles.[41] In general, the combustion efficiencies of LDGVs in China have gradually improved. The changes in MCE shown in Figure 4(a) are consistent with the actual situation in China.

NH_3 EFs can be predicted using Formula 3 and the measured MCEs. Figure 4(b) shows predicted NH_3 EFs for in-use LDGVs under different emission standards. t test was used for significant evaluation for the predicted NH_3 EFs. There was no significant difference between Euro 1 and Euro 2 vehicles, but the difference was significant with Euro 3, Euro 4, and Euro 5 vehicles, and the P values were far less than 0.01. NH_3 EFs generally decrease with more stringent emission standards. The average NH_3 EFs for Euro 1 and Euro 2 LDGVs are similar at 32.9 ± 21.7 and 30.8 ± 22.6 $mg \cdot km^{-1}$, respectively. The NH_3 EFs for Euro 3, Euro 4, and Euro 5 LDGVs have decreased by 39%, 59%, and 65%, respectively, compared with Euro 2 vehicles. NO_x emissions have decreased more rapidly

DOI: 10.1021/acs.est.8b03984
Environ. Sci. Technol. 2018, 52, 11223−11231

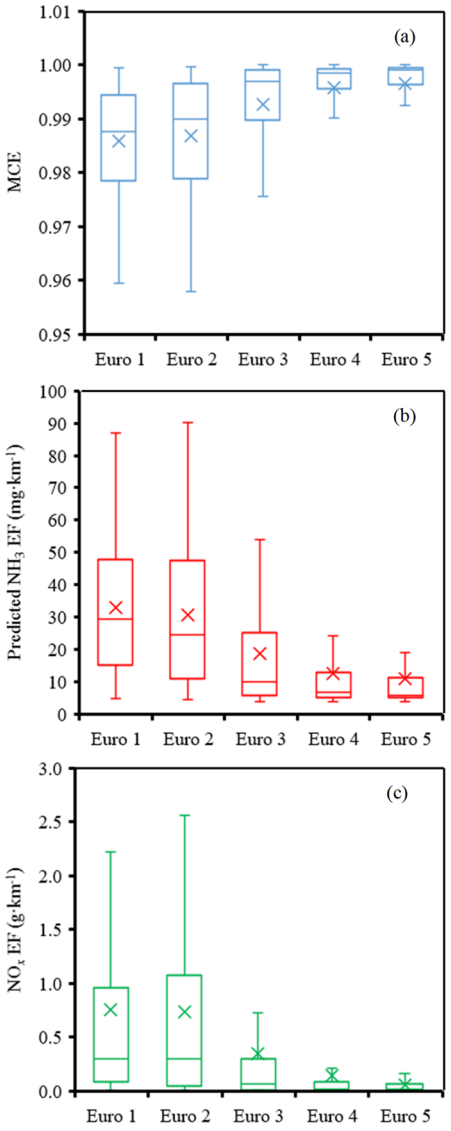

Figure 4. Box plot of (a) MCEs, (b) predicted NH_3 EFs, and (c) measured NO_x EFs for in-use LDGVs under different emission standard categories based on inspection data over the ECE cycle test. Boxes represent the 25% and 75% confidence intervals; crosses represent average values.

than NH_3 emissions. The NO_x EFs for Euro 3, Euro 4, and Euro 5 LDGVs are 52%, 81%, and 92% lower than those for Euro 2 vehicles. Following the changes in emission standards in China since 2011 (Euro 0, 1, 2, 3, and 4 vehicles accounted for 10%, 17%, 20%, 48%, and 6% in 2011, while Euro 0, 1, 2, 3, 4, and 5 vehicles accounted for 1%, 5%, 6%, 24%, 52%, and 11% in 2016), the average LDGV NH_3 and NO_x EFs were 32% and 45% lower in 2016 than in 2011. This trend is consistent with remote sensing and tunnel studies in the U.S. by Bishop et al.[12,13] and Kean et al.[16] Air-fuel ratio is the most important factor determining NH_3 generation. Better fueling control and less fuel-rich combustion in newer vehicles determine the constant decrease in NH_3 emissions. Catalytic formulation used in TWC is another factor to influence the NH_3 generation. A previous study reported that low precious metal loading TWC and lean NO_x trap (LNT) catalyst produce lower NH_3 emissions, while all of the formulations produced significant amounts of NH_3 when operated under sufficiently rich conditions.[43] Therefore, improvement of combustion efficiency dominates the reduction of NH_3 emissions in these years, which indicates that China's vehicle pollution prevention and control policies have synergistic effects in controlling NH_3 emissions from LDGVs. However, NH_3 is becoming a major contributor to nitrogen emissions, as its decreasing trend is slower than NO_x. Thus, increased monitoring of NH_3 emissions from LDGVs in China is warranted.

Because the ECE cycle does not represent actual light-duty vehicle driving conditions, we used formula (4) to predict NH_3 EFs for a number of different driving cycles, including six dynamometer cycles and two real-world cycles. The dynamometer cycles included the ECE, NEDC, FTP, UC, US06, and WLTC; the real-world cycles were obtained from an on-road driving survey in Shanghai, China.[6] A total of 150 h of valid GPS data was used to establish VSP bins on urban and highway roads, on which the average speeds were 25 and 70 $km \cdot h^{-1}$, respectively. Detailed VSP distributions for these driving cycles are provided in SI Section S6.

Figure 5 shows the predicted NH_3 EFs for different driving cycles compared with dynamometer measurements from

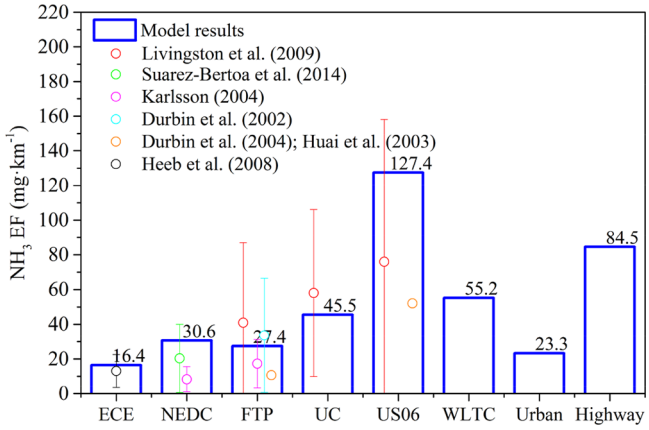

Figure 5. Predicted NH_3 EFs (blue bars) during different driving cycles and compared with dynamometer measurement results from previous studies (dots).

previous studies. The results indicate that LDGV NH_3 emissions are strongly dependent on driving conditions. The predicted NH_3 EFs are highest during the US06 cycle, followed by the WLTC, UC, NEDC, and FTP test, and lowest during the ECE cycle. The predicted NH_3 EF during the real-world urban cycle in China is 23.3 $mg \cdot km^{-1}$, similar to that measured in an urban tunnel in Shanghai, China.[8] During the highway cycle, the EF reaches 84.5 $mg \cdot km^{-1}$, or ~3.6 times that during the urban cycle. The results predicted for the ECE, NEDC, FTP, and UC tests agree well with dynamometer measurements in previous studies.[17−19,22,23,31,32] The U06 cycle predicted NH_3 EF is somewhat overestimated, but still below the upper limit of the measured results.

Uncertainty Analysis. The measured results indicate that LDGV NH_3 emissions vary widely even in vehicles with the same emission standard. Therefore, considerable uncertainty remains in the model results. Combustion efficiency is a key factor in model result uncertainty. As shown in Figure 4(b), a lack of MCE data for individual vehicles may cause deviations of up to 103% in the predicted NH_3 EF. In contrast, the uncertainty of the 95% confidence interval is approximately

DOI: 10.1021/acs.est.8b03984
Environ. Sci. Technol. 2018, 52, 11223−11231

Table 2. NH_3 EFs Predicted by Different Vehicle Emission Models

	urban (mg·km^{-1})					highway (mg·km^{-1})				
models	Euro 1	Euro 2	Euro 3	Euro 4	Euro 5	Euro 1	Euro 2	Euro 3	Euro 4	Euro 5
this study	46	43	25	16	13	168	156	91	57	47
MOVES 2014a	71	55	32	13	12	36	27	11	6	6
COPERT 4v5.1	70	176	2	2	0	63	59	73	73	0
IVE v2.0	59	59	60	63	N/A	64	65	66	69	N/A

54% when the MCE is known, according to Figure 3. Other factors, including TWC efficiency,[18] environmental temperature,[31] and even fuel quality,[19] also influence model accuracy. Nevertheless, the NH_3 EFs predicted herein generally agree well with the existing field measurement results and can represent the overall LDGV NH_3 emissions in China.

Comparison to Existing Vehicle Emission Models. Existing vehicle emission models, such as MOVES, COPERT, and IVE, can also be used to predict LDGV NH_3 emissions. To compare these models to the model presented herein, we used these models to calculate NH_3 EFs for Euro 1 through Euro 5 LDGVs under both urban and highway cycles in Shanghai, China. Because the MOVES model calculates vehicle emissions based on the model year instead of the emission standard, we used the years in which Euro 1 through Euro 5 were implemented, namely 1992, 1996, 2000, 2005, and 2010, respectively, to represent the equivalent emission standards. Table 2 compares the NH_3 EFs predicted by these models and the model presented herein. The trends predicted by our model between NH_3 EFs and emission standards are consistent with those predicted by MOVES. However, MOVES predicts much lower EFs during the highway cycle than does the model herein. The average NH_3 EFs and EF-emission standard relationships predicted by COPERT and IVE models are quite different from those predicted by our model. Overall, the LDGV NH_3 emissions estimated in China by existing models deviate considerably. First, the MOVES and COPERT models estimate smaller values of NH_3 emissions compared with our model results, while IVE model estimates larger values relative. Second, the COPERT and IVE models do not accurately reflect the trends in LDGV NH_3 emissions as China continues to accelerate its fleet composition updates.

Implications. NH_3 from vehicles is an important source of secondary aerosols in the urban atmosphere in China.[8−10] However, NH_3 emissions from LDGVs in China are not well constrained due to a lack of measurements. The number of gasoline vehicles reached 0.16 billion by the end of 2016, increasing at a rate of more than 15% per year. If an annual mileage of 15 000 km is assumed for each LDGV, the estimated NH_3 emissions from LDGVs in China would be approximately 0.12 Mt based on the EFs predicted in this study. The total LDGV NH_3 emissions are far below those from agricultural sources (which were recently estimated to be ∼8 Mt in 2012).[26] However, they dominate the NH_3 emissions in urban areas, especially during morning and evening peak-traffic hours, when agricultural emissions are relatively low.[42]

In addition, we found higher LDGV NH_3 emissions under aggressive highway driving cycles. Recent rapid growth in urbanization and economic scale in China have led to extensive highway development and greatly increased intercity vehicular traffic. For example, in Shanghai, light-duty vehicle highway mileage accounts for ∼48% of the total mileage traveled. The average LDGV NH_3 EF during a comprehensive driving cycle is estimated to be 52.7 mg·km^{-1}, more than 2 times that during an urban cycle. Therefore, accounting only for NH_3 emissions on urban roads will lead to considerable underestimation of emissions.

It is worth mentioning that LDGV NH_3 emissions have decreased in conjunction with the effective implementation of vehicle emission control policies in China. China will continue to accelerate the refurbishment and elimination of old vehicles, which should in turn promote decreases in LDGV NH_3 emissions in China within the next few years. However, motor vehicles remain a notable source of NH_3 in urban areas due to accelerated urbanization and car use in China. This study provides a detailed EF data set that can be used to compile vehicular NH_3 emission inventories and predict future trends in vehicular NH_3 emissions in China.

■ ASSOCIATED CONTENT

Supporting Information

The Supporting Information is available free of charge on the ACS Publications website at DOI: 10.1021/acs.est.8b03984.

Specifications, emission factors, and fuel consumption for the test vehicles; NH_3 emissions reproducibility test data; the effect of cold-start conditions on NH_3 emissions; emission factors for different emission standard categories; VSP distributions for different driving cycles; Figures S1−S5; and Table S1 (PDF)

■ AUTHOR INFORMATION

Corresponding Authors

*(C.H.) Phone: +86 64085119; fax: +86 64085119; e-mail: huangc@saes.sh.cn.

*(L.L.) Phone: +86 64085119; fax: +86 64085119; e-mail: lili@saes.sh.cn.

ORCID

Cheng Huang: 0000-0001-9518-3628

Li Li: 0000-0001-5575-0894

Present Address

¶Institute of Environmental Pollution and Health, Shanghai University, Shanghai, 200244, China.

Notes

The authors declare no competing financial interest.

■ ACKNOWLEDGMENTS

This work was supported by the National Key R&D Program of China (No. 2017YFC0212101), the National Natural Science Foundation of China (Grant No. 21777101), and the Shanghai Environmental Protection Bureau Fund Project (Grant No. 2018-43). We are indebted to the Hangzhou Vehicle Pollution Management Office and Hangzhou Academy of Environmental Protection Sciences for providing the vehicle emission inspection data.

DOI: 10.1021/acs.est.8b03984
Environ. Sci. Technol. 2018, 52, 11223−11231

REFERENCES

(1) Seinfeld, J. H.; Pandis, S. N. *Atmospheric Chemistry and Physics: From Air Pollution to Climate Change*, 2nd ed.; Wiley: New York, 2006, 265−266.

(2) Zhang, R.; Wang, G.; Guo, S.; Zamora, M. L.; Ying, Q.; Lin, Y.; Wang, W.; Hu, M.; Wang, Y. Formation of urban fine particulate matter. *Chem. Rev.* **2015**, *115* (10), 3803−3855.

(3) Guo, S.; Hu, M.; Zamora, M. L.; Peng, J.; Shang, D.; Zheng, J.; Du, Z.; Wu, Z.; Shao, M.; Zeng, L.; Molinac, M. J.; Zhang, R. Elucidating severe urban haze formation in China. *Proc. Natl. Acad. Sci. U. S. A.* **2014**, *111* (49), 17373−17378.

(4) Paulot, F.; Jacob, D. J.; Pinder, R. W.; Bash, J. O.; Travis, K.; Henze, D. K. Ammonia emissions in the United States, European Union, and China derived by high-resolution inversion of ammonium wet deposition data: Interpretation with a new agricultural emissions inventory (MASAGE_NH_3). *J. Geophys. Res. Atmos.* **2014**, *119*, 4343−4364.

(5) Huang, X.; Song, Y.; Li, M. M.; Li, J. F.; Huo, Q.; Cai, X. H.; Zhu, T.; Hu, M.; Zhang, H. S. A high-resolution ammonia emission inventory in China. *Global Biogeochem. Cycles.* **2012**, *26*, GB1030.

(6) Huang, C.; Chen, C. H.; Li, L.; Cheng, Z.; Wang, H. L.; Huang, H. Y.; Streets, D. G.; Wang, Y. J.; Zhang, G. F.; Chen, Y. R. Emission inventory of anthropogenic air pollutants and VOC species in the Yangtze River Delta region, China. *Atmos. Chem. Phys.* **2011**, *11* (9), 4105−4120.

(7) Zheng, J. Y.; Yin, S. S.; Kang, D. W.; Che, W. W.; Zhong, L. J. Development and uncertainty analysis of a high-resolution NH_3 emissions inventory and its implications with precipitation over the Pearl River Delta region, China. *Atmos. Chem. Phys.* **2012**, *12* (15), 7041−7058.

(8) Chang, Y. H.; Zhou, Z.; Deng, C. R.; Huang, K.; Collett, J. L.; Lin, J.; Zhuang, G. S. The importance of vehicle emissions as a source of atmospheric ammonia in the megacity of Shanghai. *Atmos. Chem. Phys.* **2016**, *16* (5), 3577−3594.

(9) Sun, K.; Tao, L.; Miller, D. J.; Pan, D.; Golston, L. M.; Zondlo, M. A.; Griffin, R. J.; Wallace, H. W.; Leong, Y. J.; Yang, M. M.; Zhang, Y.; Mauzerall, D. L.; Zhu, T. Vehicle emissions as an important urban ammonia source in the United States and China. *Environ. Sci. Technol.* **2017**, *51* (4), 2472−2481.

(10) Pan, Y.; Tian, S.; Liu, D.; Fang, Y.; Zhu, X.; Zhang, Q.; Zheng, B.; Michalski, G.; Wang, Y. Fossil fuel combustion-related emissions dominate atmospheric ammonia sources during severe haze episodes: Evidence from ^{15}N-stable isotope in size-resolved aerosol ammonium. *Environ. Sci. Technol.* **2016**, *50* (15), 8049−8056.

(11) Shelef, M.; Gandhi, H. S. Ammonia formation in the catalytic reduction of nitric Oxide. III. The role of water gas shift, reduction by hydrocarbons, and steam reforming. *Ind. Eng. Chem. Prod. Res. Dev.* **1974**, *13* (1), 80−85.

(12) Bishop, G. A.; Peddle, A. M.; Stedman, D. H.; Zhan, T. On-road emission measurements of reactive nitrogen compounds from three California cities. *Environ. Sci. Technol.* **2010**, *44* (9), 3616−3620.

(13) Bishop, G. A.; Stedman, D. H. Reactive nitrogen species emission trends in three light-/medium- duty United States fleets. *Environ. Sci. Technol.* **2015**, *49* (18), 11234−11240.

(14) Fraser, M. P.; Cass, G. R. Detection of Excess ammonia emissions from in-use vehicles and the implications for fine particle control. *Environ. Sci. Technol.* **1998**, *32* (8), 1053−1057.

(15) Kean, A. J.; Harley, R. A.; Littlejohn, D.; Kendall, G. R. On-road measurement of ammonia and other motor vehicle exhaust emissions. *Environ. Sci. Technol.* **2000**, *34* (17), 3535−3539.

(16) Kean, A. J.; Littlejohn, D.; Ban-Weiss, G. A.; Harley, R. A.; Kirchstetter, T. W.; Lunden, M. M. Trends in on-road vehicle emissions of ammonia. *Atmos. Environ.* **2009**, *43* (8), 1565−1570.

(17) Durbin, T. D.; Wilson, R. D.; Norbeck, J. M.; Miller, J. W.; Huai, T.; Rhee, S. H. Estimates of the emission rates of ammonia from light-duty vehicles using standard chassis dynamometer test cycles. *Atmos. Environ.* **2002**, *36* (9), 1475−1482.

(18) Huai, T.; Durbin, T. D.; Miller, J. W.; Pisano, J. T.; Sauer, C. G.; Rhee, S. H.; Norbeck, J. M. Investigation of NH_3 emissions from new technology vehicles as a function of vehicle operating conditions. *Environ. Sci. Technol.* **2003**, *37* (21), 4841−4847.

(19) Durbin, T. D.; Pisano, J. T.; Younglove, T.; Sauer, C. G.; Rhee, S. H.; Huai, T.; Miller, J. W.; MacKay, G. I.; Hochhauser, A. M.; Ingham, M. C.; Gorse, R. A., Jr.; Beard, L. K.; DiCicco, D.; Thompson, N.; Stradling, R. J.; Rutherford, J. A.; Uihlein, J. P. The effect of fuel sulfur on NH_3 and other emissions from 2000−2001 model year vehicles. *Atmos. Environ.* **2004**, *38* (17), 2699−2708.

(20) Huai, T.; Durbin, T. D.; Younglove, T.; Scora, G.; Barth, M.; Norbeck, J. M. Vehicle specific power approach to estimating on-road NH_3 emissions from light-duty vehicles. *Environ. Sci. Technol.* **2005**, *39* (24), 9595−9600.

(21) Heeb, N. V.; Forss, A. M.; Brühlmann, S.; Lüscher, R.; Saxer, C. J.; Hug, P. Three-way catalyst-induced formation of ammonia velocity- and acceleration-dependent emission factors. *Atmos. Environ.* **2006**, *40* (31), 5986−5997.

(22) Heeb, N. V.; Saxer, C. J.; Forss, A.; Brühlmann, S. Trends of NO-, NO_2-, and NH_3- emissions from gasoline-fueled Euro-3- to Euro-4-passenger cars. *Atmos. Environ.* **2008**, *42* (10), 2543−2554.

(23) Livingston, C.; Rieger, P.; Winer, A. Ammonia emissions from a representative in-use fleet of light and medium-duty vehicles in the California South Coast Air Basin. *Atmos. Environ.* **2009**, *43* (21), 3326−3333.

(24) Liu, T.; Wang, X.; Wang, B.; Ding, X.; Deng, W.; Lü, S.; Zhang, Y. Emission factor of ammonia (NH_3) from on-road vehicles in China: tunnel tests in urban Guangzhou. *Environ. Res. Lett.* **2014**, *9* (6), 064027.

(25) Sun, K.; Tao, L.; Miller, D. J.; Khan, M. A.; Zondlo, M. A. On-road ammonia emissions characterized by mobile, open-path measurements. *Environ. Sci. Technol.* **2014**, *48* (7), 3943−3950.

(26) Kang, Y. N.; Liu, M. X.; Song, Y.; Huang, X.; Yao, H.; Cai, X. H.; Zhang, H. S.; Kang, L.; Liu, X. J.; Yan, X. Y.; He, H.; Zhang, Q.; Shao, M.; Zhu, T. High-resolution ammonia emissions inventories in China from 1980 to 2012. *Atmos. Chem. Phys.* **2016**, *16* (4), 2043−2058.

(27) Tang, G. Q.; Chao, N.; Wang, Y. S.; Chen, J. S. Vehicular emissions in China in 2006 and 2010. *J. Environ. Sci.* **2016**, *48*, 179−192.

(28) Lang, J. L.; Zhou, Y.; Cheng, S. Y.; Zhang, Y. Y.; Dong, M.; Li, S. Y.; Wang, G.; Zhang, Y. L. Unregulated pollutant emissions from on-road vehicles in China, 1999−2014. *Sci. Total Environ.* **2016**, *573*, 974−984.

(29) Meng, W. J.; Zhong, Q. R.; Yun, X.; Zhu, X.; Huang, T. B.; Shen, H. Z.; Chen, Y. L.; Chen, H.; Zhou, F.; Liu, J. F.; Wang, X. M.; Zeng, E. Y.; Tao, S. Improvement of a global high-resolution ammonia emission inventory for combustion and industrial sources with new data from the residential and transportation sectors. *Environ. Sci. Technol.* **2017**, *51* (5), 2821−2829.

(30) Ministry of Environmental Protection of the People's Republic of China (MEP). China vehicle environmental management annual report 2017. *Vehicle Emission Control Center of MEP*, Beijing, 2017, 1−4.

(31) Suarez-Bertoa, R.; Zardini, A. A.; Astorga, C. Ammonia exhaust emissions from spark ignition vehicles over the New European Driving Cycle. *Atmos. Environ.* **2014**, *97* (SI), 43−53.

(32) Karlsson, H. L. Ammonia, nitrous oxide and hydrogen cyanide emissions from five passenger vehicles. *Sci. Total Environ.* **2004**, *334*−*335*, 125−132.

(33) Vieira-Filho; Marcelo, S.; Ito, D. T.; Pedrotti, J. J.; Coelho, L. H. G.; Fornaro, A. Gas-phase ammonia and water-soluble ions in particulate matter analysis in an urban vehicular tunnel. *Environ. Sci. Pollut. Res.* **2016**, *23*, 19876−19886.

(34) Baum, M. M.; Kiyomiya, E. S.; Kumar, S.; Lappas, A. M.; Kapinus, V. A.; Lord, H. C., III. Multicomponent remote sensing of vehicle exhaust by dispersive absorption spectroscopy. 2. Direct on-road ammonia measurements. *Environ. Sci. Technol.* **2001**, *35* (18), 3735−3741.

DOI: 10.1021/acs.est.8b03984
Environ. Sci. Technol. 2018, 52, 11223−11231

(35) Burgard, D. A.; Bishop, G. A.; Stedman, D. H. Remote Sensing of Ammonia and Sulfur Dioxide from On-Road Light Duty Vehicles. *Environ. Sci. Technol.* **2006**, *40* (22), 7018−7022.
(36) Zavala, M.; Herndon, S. C.; Slott, R. S.; Dunlea, E. J.; Marr, L. C.; Shorter, J. H.; Zahniser, M.; Knighton, W. B.; Rogers, T. M.; Kolb, C. E.; Molina, L. T.; Molina, M. J. Characterization of on-road vehicle emissions in the Mexico City Metropolitan Area using a mobile laboratory in chase and fleet average measurement modes during the MCMA-2003 field campaign. *Atmos. Chem. Phys.* **2006**, *6*, 5129−5142.
(37) Carslaw, D. C.; Rhys-Tyler, G. New insights from comprehensive on-road measurements of NO_x, NO_2 and NH_3 from vehicle emission remote sensing in London, UK. *Atmos. Environ.* **2013**, *81*, 339−347.
(38) Jimenez-Palacios, J. L. *Understanding and Quantifying Motor Vehicle Emissions with Vehicle Specific Power and TILDAS Remote Sensing*; Ph. D. Thesis, Massachusetts Institute of Technology: Cambridge, MA, 1999.
(39) Bradow, R. L.; Stump, F. D. Unregulated Emissions from Three-way Catalyst Cars. *SAE Tech. Pap. Ser.* **1977**, 770369.
(40) Wu, Y.; Zhang, S. J.; Hao, J. M.; Liu, H.; Wu, X. M.; Hu, J. N.; Walsh, M. P.; Wallington, T. J.; Zhang, K. M.; Stevanovic, S. On-road vehicle emissions and their control in China: A review and outlook. *Sci. Total Environ.* **2017**, *574*, 332−349.
(41) Huang, C.; Tao, S. K.; Lou, S. R.; Hu, Q. Y.; Wang, H. L.; Wang, Q.; Li, L.; Wang, H. Y.; Liu, J. G.; Quan, Y. F.; Zhou, L. L. Evaluation of emission factors for light-duty gasoline vehicles based on chassis dynamometer and tunnel studies in Shanghai, China. *Atmos. Environ.* **2017**, *169*, 193−203.
(42) Zhu, L.; Henze, D.; Bash, J.; Jeong, G. R.; Cady-Pereira, K.; Shephard, M.; Luo, M.; Paulot, F.; Capps, S. Global evaluation of ammonia bidirectional exchange and livestock diurnal variation schemes. *Atmos. Chem. Phys.* **2015**, *15* (22), 12823−12843.
(43) DiGiulio, C. D.; Pihl, J. A.; Parks, J. E., II; Amiridis, M. D.; Toops, T. J. Passive-ammonia selective catalytic reduction (SCR): Understanding NH_3 formation over close-coupled three way catalysts (TWC). *Catal. Today* **2014**, *231* (4), 33−45.

DOI: 10.1021/acs.est.8b03984
Environ. Sci. Technol. 2018, 52, 11223−11231